Two Anhydrous Zeolite X Crystal Structures, $Pd_{18}Tl_{56}Si_{100}Al_{92}O_{384}$ and $Pd_{21}Tl_{50}Si_{100}Al_{92}O_{384}$

Bo Young Yoon, Mee Kyung Song, Seok Hee Lee, and Yang Kim*

Department of Chemistry and Chemistry Institute for Functional Materials, Pusan National University, Pusan 609-735, Korea
Received July 25, 2000

The crystal structures of fully dehydrated Pd^{2+}- and Tl^+-exchanged zeolite X, $Pd_{18}Tl_{56}Si_{100}Al_{92}O_{384}$ ($Pd_{18}Tl_{56}$-X, a = 24.935(4) Å) and $Pd_{21}Tl_{50}Si_{100}Al_{92}O_{384}$ ($Pd_{21}Tl_{50}$-X, a = 24.914(4) Å), have been determined by single-crystal X-ray diffraction methods in the cubic space group $Fd\bar{3}$ at 21(1) °C. The crystals were prepared using an exchange solution that had a $Pd(NH_3)_4Cl_2$: $TlNO_3$ mole ratio of 50 : 1 and 200 : 1, respectively, with a total concentration of 0.05 M for 4 days. After dehydration at 360 °C and 2×10^{-6} Torr in flowing oxygen for 2 days, the crystals were evacuated at 21(1) °C for 2 hours. They were refined to the final error indices R_1 = 0.045 and R_2 = 0.038 with 344 reflections for $Pd_{18}Tl_{56}$-X, and R_1 = 0.043 and R_2 = 0.045 with 280 reflections for $Pd_{21}Tl_{50}$-X; $I > 3\sigma(I)$. In the structure of dehydrated $Pd_{18}Tl_{56}$-X, eighteen Pd^{2+} ions and fourteen Tl^+ ions are located at site I′. About twenty-seven Tl^+ ions occupy site II recessed 1.74 Å into a supercage from the plane of three oxygens. The remaining fifteen Tl^+ ions are distributed over two non-equivalent III′ sites, with occupancies of 11 and 4, respectively. In the structure of $Pd_{21}Tl_{50}$-X, twenty Pd^{2+} and ten Tl^+ ions occupy site I′, and one Pd^{2+} ion is at site I. About twenty-three Tl^+ ions occupy site II, and the remaining seventeen Tl^+ ions are distributed over two different III′ sites. Pd^{2+} ions show a limit of exchange (*ca.* 39% and 46%), though their concentration of exchange was much higher than that of Tl^+ ions. Pd^{2+} ions tend to occupy site I′, where they fit the double six-ring plane as nearly ideal trigonal planar. Tl^+ ions fill the remaining I′ sites, then occupy site II and two different III′ sites. The two crystal structures show that approximately two and one-half I′ sites per sodalite cage may be occupied by Pd^{2+} ions. The remaining I′ sites are occupied by Tl^+ ions with Tl-O bond distance that is shorter than the sum of their ionic radii. The electrostatic repulsion between two large Tl^+ ions and between Tl^+ and Pd^{2+} ions in the same β-cage pushes each other to the charged six-ring planes. It causes the Tl-O bond to have some covalent character. However, Tl^+ ions at site II form ionic bonds with three oxygens because the supercage has the available space to obtain the reliable ionic bonds.

Keywords: Structure, Zeolite X, Thallium, Palladium, Ion-exchange.

Introduction

Zeolites have been widely used in industrial applications as ion exchangers, sorbents, and catalysts.[1,2] Because the structural stability and catalytic properties of zeolites depend on the type and number of cations and distribution over the available sites, determining the cationic positions and occupancies in various ion exchanged zeolites can be useful. Recent single-crystal X-ray studies of zeolites have shown that the extra-framework structures, especially the cation distribution, may be rationalized in terms of the sizes, charges, and the electronic natures of the exchanged cations.

Transition metal ions can coordinate to guest molecules more selectively than filled-shell cations and often reach other oxidation states easily. Thus, the introduction of transition metals into zeolites induces new catalytic activity.[2] They can be introduced by ion-exchange.[3-9] However, the results are not always simple. Only a fraction of the original cations, Na^+ ions, can be replaced, and a relatively sharp upper limit to exchange has been observed.[4,5] If the exchanging cation can hydrolyze, the H^+ concentration in a solution may increase, encouraging H^+ exchange and finally leading to the modification, destruction, or dissolution of the zeolite framework. In order to understand the catalytic properties of zeolites containing the more complex transition metal ions, it is useful to establish the positions and occupancies of ions within the zeolites cavities. In particular, Pd-containing zeolites prepared by ion exchange in a solution have been studied extensively.[10-14] A complete description of the palladium position in Pd-Y zeolites has been given as a function of O_2 activation at various temperatures.[15] At temperatures below 250 °C, supercage $Pd(NH_3)_4^{2+}$ ions lose ammonia to form $Pd(NH_3)_2^{2+}$ ions that are coordinated to lattice oxygen atoms. At higher temperatures, these ions decompose to $Pd(NH_3)^{2+}$ or Pd^{2+}, which move into the sodalite cages, where they are stabilized by electrostatic interactions and by the higher coordination with framework oxygen atoms.[16,17] This is attributed to the higher negative charge density in this cavity.[17] Recently, the crystal structures of partially Pd^{2+}-exchanged zeolite X dehydrated in oxygen at 400 °C have been determined.[18] The linear $[HO\text{-}Pd\text{-}O\text{-}Pd\text{-}OH]^{4+}$ clusters passing through the center of a double six-ring (D6R) and extending into its two adjacent sodalite cavities have been found. The formation of linear Pd_2O_3 clusters in the sodalite cavity may be an impressive phenomenon for solid state chemists.

Kim *et al.* studied the crystal structure of dehydrated Tl^+-exchanged zeolite X.[19] In Tl_{92}-X, 92 Tl^+ ions are distributed in four different crystallographic sites: I′ in the sodalite cavity on a three-fold axis, II in the supercage, and two crystallographically different III′ sites. Tl^+ ions are too large to occupy site I, the center of the double six-ring.

Several structural studies of monovalent and divalent ion exchanged zeolites A and X have been reported[7,20-22] seeing the site selectivity of various cations. The structures of fully dehydrated $Ca_{32}K_{28}$-X[20], $Ca_{31}Rb_{30}$-X[21], $Cd_{24.5}Tl_{43}$-X[7], $Sr_{31}K_{30}$-X[22], and $Sr_{8.5}Tl_{75}$-X[22] were determined. In these structures, the small and highly charged Cd^{2+}, Ca^{2+}, and Sr^{2+} ions tend to occupy site I, with the remainder going to site II. The large Tl^+ and K^+ ions, which are less able to balance the anionic charge of the zeolite framework than the small and highly charged divalent ions, can fill the double six-ring with some occupancies at site I′ and finish filling site II, with the remainder of them going to the least suitable cationic sites in the structure, sites III and III′.

The present study was conducted to find the location of cations within the zeolite framework. The fully dehydrated structures of $Pd_{18}Tl_{56}$-X and $Pd_{21}Tl_{50}$-X are presented. The occupancy numbers, selective positions, and the coordination environment of Pd^{2+} and Tl^+ ions are investigated.

Experimental Section

Crystal Preparation. Large single crystals of sodium zeolite X, $Na_{92}Si_{100}Al_{92}O_{384}$, were prepared in St. Petersburg, Russia.[23] A colorless octahedron with a cross-section of about 0.2 mm was lodged in a fine Pyrex capillary for the ion exchange. $Pd_{18}Tl_{56}$-X and $Pd_{21}Tl_{50}$-X were prepared by using an exchange solution that had a $Pd(NH_3)_4Cl_2$: $TlNO_3$ mole ratio of 50 : 1 and 200 : 1, respectively, with a total concentration of 0.05 M. The solution was allowed to flow past the crystal at a velocity of approximately 15 mm/s for 4 days at 21(1) °C. To avoid Pd° metal clusters, which could be difficult to locate crystallographically, the crystals were dehydrated at 360 °C and 2×10^{-6} Torr for 2 days in a flowing stream of oxygen gas (790 Torr). Then, each crystal was allowed to cool and was evacuated at room temperature and 2×10^{-6} Torr for 2 hours. After cooling to room temperature, each crystal, still under vacuum, was sealed in its capillary by a torch. The crystals became dark orange in color.

X-Ray Data Collection. The cubic space group $Fd\bar{3}$ was used throughout this study. This was justified by the low Si/Al ratio, which in turn requires, at least in the short range, alternation of Si and Al, and by the observation that this crystal, like all other crystals from the same batch, did not have intensity symmetry across (110) and therefore lacked that mirror plane. Diffraction data were collected with an automated four-circle CAD-4 diffractometer equipped with a pulse-height analyzer and a graphite monochromator. Molybdenum radiation was used for all experiments ($K\alpha_1$, λ = 0.70930 Å; $K\alpha_2$, λ = 0.71359 Å). The cubic unit cell constants, a, which were determined at 21(1) °C by a least-squares refinement of 25 intense reflections for which $14° < 2\theta < 22°$, are 24.935(4) Å and 24.914(4) Å for $Pd_{18}Tl_{56}$-X and $Pd_{21}Tl_{50}$-X, respectively. All unique reflections in the positive octant of an F-centered unit cell for which $2\theta < 50°$, $l > h$, and $k > h$ were recorded. Of the 1,392 unique reflections measured for $Pd_{18}Tl_{56}$-X and 1,386 reflections for $Pd_{21}Tl_{50}$-X, only 344 and 280 reflections for the respective structures for which $I > 3\sigma(I)$ were used in the subsequent structure determinations. Spherical absorption corrections (for the $Pd_{18}Tl_{56}$-X, μR = 1.55 and ρ_{cal} = 2.654 g/cm^3; for the $Pd_{21}Tl_{50}$-X, μR = 1.41 and ρ_{cal} = 2.563 g/cm^3) were applied.[24] The calculated transmission coefficients ranged from 0.09 to 0.11 for both crystals. These corrections had little effect on the final R indices. Other details of the data collection have been reported previously.[25]

Structure Determination

$Pd_{18}Tl_{56}$-X: A full-matrix least-squares refinement was initiated by using the atomic positions of the framework atoms [Si, Al, O(1), O(2), O(3), and O(4)] in dehydrated $Pd_{30}Na_{32}$-X.[18] Anisotropic refinement converged to an unweighted error index R_1, $(\Sigma(F_o-|F_c|)/\Sigma F_o)$, of 0.57, and a weighted error index R_2, $(\Sigma w(|F_o-|F_c||)^2/\Sigma w F_o^2)^{1/2}$, of 0.65.

A difference Fourier function revealed two large peaks at (0.253, 0.253, 0.253) and (0.07, 0.07, 0.07), with peak heights of 19.3 eÅ^{-3} and 12.5 eÅ^{-3}, respectively. It is easy to distinguish Pd^{2+} from Tl^+ because of their large difference in atomic scattering factors (44 e$^-$ for Pd^{2+} and 80 e$^-$ for Tl^+) and in ionic radii (Pd^{2+} = 0.86 Å and Tl^+ = 1.47 Å).[26] Also, the approach distances between Tl^+ ions and oxygens in the zeolite framework in dehydrated Tl_{92}-X have been determined[19] and are indicative. Anisotropic refinement, including these as Tl^+ ions at Tl(2) and Tl(1), converged to R_1 = 0.17 and R_2 = 0.23, with occupancies of 26.8(1) and 14.9(1) per unit cell, respectively. A subsequent difference Fourier synthesis revealed a peak at Pd(1), (0.047, 0.047, 0.047), of height 13.6 eÅ^{-3}. An anisotropic refinement of the framework atoms, Pd(1), Tl(1), and Tl(2) (see Table 1) converged to R_1 = 0.11 and R_2 = 0.15.

A subsequent difference Fourier synthesis showed peaks at Tl(3), (0.41, 0.11, 0.13), and at Tl(4), (0.41, 0.07, 0.07), with peak heights 7.6 eÅ^{-3} and 2.7 eÅ^{-3}, respectively. An anisotropic refinement of the framework atoms, Pd(1), Tl(1), Tl(2), Tl(3), and Tl(4) converged to R_1 = 0.044 and R_2 = 0.040. Considering the cationic charge per unit cell, the occupancies of Pd(1), Tl(1), Tl(2), Tl(3), and Tl(4) were fixed at the values shown in Table 1. The final error indices for the 344 reflections for which $I > 3\sigma(I)$ were R_1 = 0.045 and R_2 = 0.038. The shift in the final cycle of the least-squares refinement was less than 0.1% of the corresponding standard deviations. The final structural parameters and selected interatomic distances and angles are presented in Tables 1(a) and 2, respectively.

$Pd_{21}Tl_{50}$-X: A full-matrix least-squares refinement was initiated by using the atomic parameters of the framework atoms for the crystal of $Pd_{18}Tl_{56}$-X. An anisotropic refinement converged to an unweighted error index R_1 of 0.55 and

Table 1. Positional[a], Thermal[a], and Occupancy Parameters[a]
(a) $Pd_{18}Tl_{56}$-X

Atom	Wyc. Pos.	x	y	z	[b]U_{11}	U_{22}	U_{33}	U_{12}	U_{13}	U_{23}	[c]Occupancy varied	fixed
Al	96(g)	-540(3)	369(3)	1247(3)	229(38)	161(35)	239(37)	59(35)	-51(37)	-117(35)		96
Si	96(g)	-530(3)	1253(3)	357(2)	303(40)	317(37)	157(34)	-43(38)	-13(34)	-124(35)		96
O(1)	96(g)	-1058(5)	0(7)	1027(5)	268(82)	704(97)	183(77)	-398(92)	29(65)	-200(98)		96
O(2)	96(g)	-10(8)	-18(8)	1429(6)	473(83)	497(84)	1152(126)	164(106)	-508(116)	-580(115)		96
O(3)	96(g)	-288(6)	760(6)	727(6)	448(99)	163(88)	465(106)	18(82)	-54(90)	-213(83)		96
O(4)	96(g)	-702(6)	741(6)	1777(6)	421(101)	358(96)	476(105)	-105(101)	-24(106)	-72(87)		96
Pd(1)	32(e)	416(2)	416(2)	416(2)	670(24)	670(24)	670(24)	-151(25)	-151(25)	-151(25)	18.9(3)	18
Tl(1)	32(e)	752(1)	752(1)	752(1)	375(11)	375(11)	375(11)	-1(14)	-1(14)	-1(14)	14.9(1)	14
Tl(2)	32(e)	2556(1)	2556(1)	2556(1)	377(4)	377(4)	377(4)	-22(8)	-22(8)	-22(8)	26.8(1)	27
Tl(3)	96(g)	4094(4)	1138(8)	1240(11)	233(50)	1153(127)	2393(142)	-217(87)	-231(118)	-574(94)	11.2(3)	11
Tl(4)	96(g)	4196(11)	676(14)	693(16)	388(163)	839(241)	1048(253)	-156(181)	-225(185)	32(210)	5.0(3)	4

(b) $Pd_{21}Tl_{50}$-X

Atom	Wyc. Pos.	x	y	z	[b]U_{11} or [d]U_{iso}	U_{22}	U_{33}	U_{12}	U_{13}	U_{23}	[c]Occupancy varied	fixed
Al	96(g)	-542(3)	363(3)	1249(40)	249(40)	252(40)	309(41)	56(37)	-152(40)	-137(40)		96
Si	96(g)	-525(3)	1250(3)	351(3)	239(38)	309(38)	218(36)	-114(38)	-8(36)	-124(37)		96
O(1)	96(g)	-1064(6)	-18(8)	1018(6)	369(98)	624(108)	344(92)	73(118)	139(78)	-248(116)		96
O(2)	96(g)	-19(9)	-8(9)	1436(7)	538(102)	614(104)	1461(171)	119(122)	-420(145)	-512(143)		96
O(3)	96(g)	-276(7)	768(7)	720(7)	510(113)	438(114)	515(122)	-158(95)	-151(99)	-31(99)		96
O(4)	96(g)	-688(7)	764(7)	1783(7)	662(129)	454(112)	586(122)	37(121)	-113(122)	-313(97)		96
Pd(1)	32(e)	417(2)	417(2)	417(2)	633(20)	633(20)	633(20)	-166(21)	-166(21)	-166(21)	20.0(2)	20
Pd(2)	16(c)	0	0	0	117(138)						1.0(1)	1
Tl(1)	32(e)	757(2)	757(2)	757(2)	516(20)	516(20)	516(20)	48(24)	48(24)	48(24)	10.5(1)	10
Tl(2)	32(e)	2565(1)	2565(1)	2565(1)	448(6)	448(6)	448(6)	-1(10)	-1(10)	-1(10)	23.1(1)	23
Tl(3)	96(g)	4098(3)	1175(11)	1260(13)	256(47)	1801(121)	2005(115)	-584(105)	602(119)	-902(82)	12.6(2)	13
Tl(4)	96(g)	4183(18)	825(27)	904(34)	797(270)	2461(566)	4998(741)	106(353)	-565(460)	2437(444)	3.8(4)	4

[a]Positional and anisotropic thermal parameters are given $\times 10^4$. Numbers in parentheses are the esd's in the units of the least significant digit given for the corresponding parameter. [b]The anisotropic temperature factor = $\exp[(-2\pi^2/a^2)(U_{11}h^2+U_{22}k^2+U_{33}l^2-U_{12}hk+U_{13}hl-U_{23}kl)]$. [c]Occupancy factors are given as the number of atoms or ions per unit cell. [d]$U_{iso} = (B_{iso}/8\pi^2)$

a weighted error index R_2 of 0.64.

A difference Fourier function revealed peaks at (0.254, 0.254, 0.254) and (0.079, 0.079, 0.079), with heights 17.5 eÅ^{-3} and 5.7 eÅ^{-3}, respectively. An anisotropic refinement, including these as Tl^+ ions at Tl(2) and Tl(1), converged to R_1 = 0.23 and R_2 = 0.30, with occupancies of 23.1(1) and 10.5(1) per unit cell, respectively. A subsequent difference Fourier function revealed two additional peaks, at (0.042, 0.042, 0.042) with a height of 15.7 eÅ^{-3}, and at (0.40, 0.12, 0.14) with a height of 6.6 eÅ^{-3}. The inclusion of these peaks as ions at Pd(1) and Tl(3) lowered the error indices to R_1 = 0.065 and R_2 = 0.066. The occupancy numbers at Pd(1) and Tl(3) refined to 20.0(2) and 12.6(2), respectively. The remaining Tl^- ions were found on an ensuring Fourier function at the Tl(4) position, (0.40, 0.08, 0.09), with a height of 4.2 eÅ^{-3}. From a successive difference Fourier function, one peak was found at (0, 0, 0), with a height of 1.4 eÅ^{-3}, that was refined as Pd(2). This peak was stable in a least-squares refinement. Simultaneous refinement of positional and isotropic thermal parameters with varied occupancy numbers converged to the error indices R_1 = 0.047 and R_2 = 0.046. Considering the cationic charge per unit cell, the occupancies of Pd(1), Pd(2), Tl(1), Tl(2), Tl(3) and Tl(4) were fixed at the values shown in Table 1. The final error indices for the 280 reflections for which $I > 3\sigma(I)$ were R_1 = 0.043 and R_2 = 0.045. The shift in the final cycle of the least-squares refinement was less than 0.1% of the corresponding standard deviations. All crystallographic calculations were made using MolEN.[27] Atomic scattering factors[28] for Si, Al, O^-, Pd^{2-}, and Tl^- were used. All scattering factors were modified to account for anomalous dispersion.[29,30] The structural parameters and the selected interatomic distances and angles are presented in Tables 1(b) and 2, respectively.

Discussion

Zeolite X is a synthetic counterpart of the naturally occurring mineral faujasite. The 14-hedron with 24 vertices, known as the sodalite cavity or a β-cage, may be viewed as the principal building block of the aluminosilicate framework of zeolite (see Figure 1). These β-cages are connected tetrahedrally at six-rings by bridging oxygens to give double

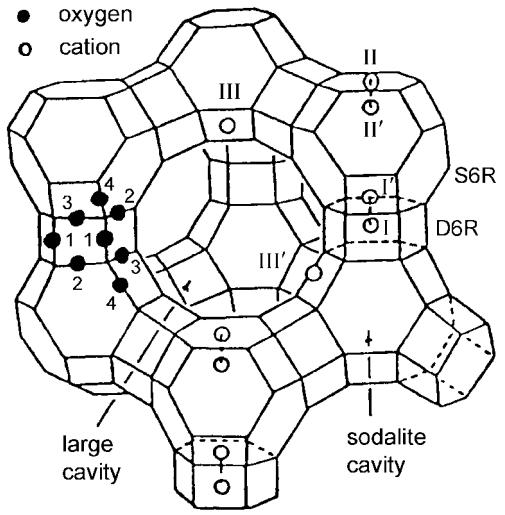

Figure 1. A stylized drawing of the framework structure of zeolite X. Near the center of the each line segment is an oxygen atom. The numbers from 1 to 4 indicates the different oxygen atoms. Silicon and aluminum atoms alternate at the tetrahedral intersections, except that a silicon atom substitutes for aluminum at about 4% of the Al positions. Extraframework cation positions are labeled with Roman numerals.

six-rings (D6R, hexagonal prism), and, also give an interconnected set of even larger cavities, supercages, accessible in three dimensions through 12-ring windows. The Si and Al atoms occupy the vertices of these polyhedra. The oxygen atoms lie approximately midway between each pair of Si and Al atoms, but are displaced from those points to give nearly tetrahedral angles about Si and Al.

Exchangeable cations, which balance the negative charge of the aluminosilicate framework, are found within the zeolite's cavities. They are usually found at the following sites shown in Figure 1: site I at the center of a D6R, I′ in the sodalite cavity on the opposite side of one of the D6R's six-rings from site I, II′ inside the sodalite cavity near a single six-ring (S6R) entrance to the supercage, II in the supercage adjacent to a S6R, III in the supercage opposite a four-ring between two 12-rings, and III′ off the twofold axis, somewhat or substantially distant from III but otherwise near the inner walls of the supercage.[31,32]

$Pd_{18}Tl_{56}$-X: The mean values of the Si-O and Al-O bond lengths are 1.62 and 1.70 Å, respectively. These values are normal. The individual bond lengths, however, show marked variations: Si-O from 1.60(2) to 1.65(2) Å, and Al-O from 1.66(2) to 1.74(2) Å. Because the Si-O and Al-O distances depend on the coordination of Pd^{2+} and Tl^{+} ions to framework oxygens of O(2) and O(3), the Si-O(2), Si-O(3), Al-O(2) and Al-O(3) bonds are somewhat lengthened (see Table 2).

In this structure, eighteen Pd^{2+} ions occupy one crystallographic site, and fifty-six Tl^{+} ions occupy four different crystallographic sites. Though the mole ratio of Pd^{2+} to Tl^{+} was 50 : 1, only 39% of the total cations were exchanged by Pd^{2+} ions. Eighteen Pd^{2+} ions at Pd(1) preferentially occupy site I′ (see Figure 2), which is a 32-fold position. The remaining

Table 2. Selected Interatomic Distance (Å) and Angles (deg)[a]

	$Pd_{18}Tl_{56}$-X	$Pd_{21}Tl_{50}$-X
Si-O(1)	1.60(2)	1.55(2)
Si-O(2)	1.63(2)	1.65(2)
Si-O(3)	1.65(2)	1.63(2)
Si-O(4)	1.61(2)	1.57(2)
Average	1.62	1.60
Al-O(1)	1.68(2)	1.71(2)
Al-O(2)	1.70(2)	1.66(2)
Al-O(3)	1.74(2)	1.79(2)
Al-O(4)	1.66(2)	1.70(2)
Average	1.70	1.72
Pd(1)-O(3)	2.10(1)	2.08(2)
Pd(2)-O(3)		2.71(2)
Tl(1)-O(3)	2.59(1)	2.58(2)
Tl(2)-O(2)	2.82(1)	2.82(2)
Tl(3)-O(4)	2.75(2)/3.02(2)	2.83(3)/2.97(3)
Tl(4)-O(1)	3.03(4)/3.07(4)	2.98(7)/3.15(7)
O(1)-Si-O(2)	112.0(1)	114.0(1)
O(1)-Si-O(3)	111.6(8)	112.4(9)
O(1)-Si-O(4)	110.2(8)	109.6(9)
O(2)-Si-O(3)	103.2(9)	103.0(1)
O(2)-Si-O(4)	108.3(8)	108.0(1)
O(3)-Si-O(4)	111.3(8)	109.8(9)
O(1)-Al-O(2)	112.0(9)	112.0(1)
O(1)-Al-O(3)	109.9(8)	110.4(8)
O(1)-Al-O(4)	112.2(8)	115.2(9)
O(2)-Al-O(3)	103.7(8)	103.0(1)
O(2)-Al-O(4)	107.1(8)	106.0(1)
O(3)-Al-O(4)	111.5(8)	108.8(9)
Si-O(1)-Al	142.3(9)	143.0(1)
Si-O(2)-Al	144.0(1)	142.0(1)
Si-O(3)-Al	135.0(1)	134.0(1)
Si-O(4)-Al	145.0(1)	148.0(1)
O(3)-Pd(1)-O(3)	119.9(6)	119.9(7)
O(3)-Pd(2)-O(3)		83.1(5)/96.9(5)/180[b]
O(3)-Tl(1)-O(3)	89.1(5)	88.6(5)
O(2)-Tl(2)-O(2)	85.7(6)	84.7(6)
O(4)-Tl(3)-O(4)	78.3(5)	76.6(5)
O(1)-Tl(4)-O(1)	115.0(1)	114.0(2)
O(1)-Tl(4)-O(4)	55.5(8)/59.5(8)	52.0(1)/63.0(7)

[a]Numbers in parentheses are estimated standard deviations in least significant digit given for the corresponding values. [b]Exactly by symmetry.

fourteen I′ sites are filled by Tl^{+} ions at Tl(1) because high negative charge density in the sodalite cavity should be transferred to the cations at site I or I′ to stabilize the structure by electrostatic interaction. Our observations showed that 75% of sodalite cavities can contain two Pd^{2+} and two Tl^{-} ions with remaining 25% containing one Tl^{-} and three Pd^{2+} ions. Each Pd(1) and Tl(1) is recessed, respectively, *ca.* 0.07 Å and 1.52 Å into the sodalite unit from its three O(3)

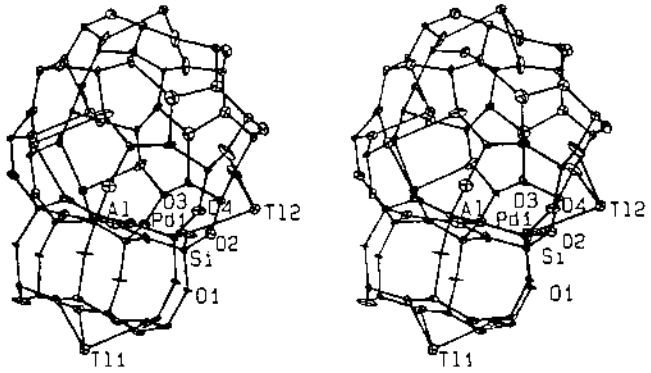

Figure 2. Stereoview of a sodalite cavity with an attached D6R in dehydrated $Pd_{18}Tl_{56}$-X. Three Pd^{2+} ions at Pd(1) (site I′), one Tl^- ion at Tl(1) (site I′) and four Tl^+ ions at Tl(2) (site II) are shown. About 25% of sodalite cavities can have this arrangement. Ellipsoids of 20 % probability are shown.

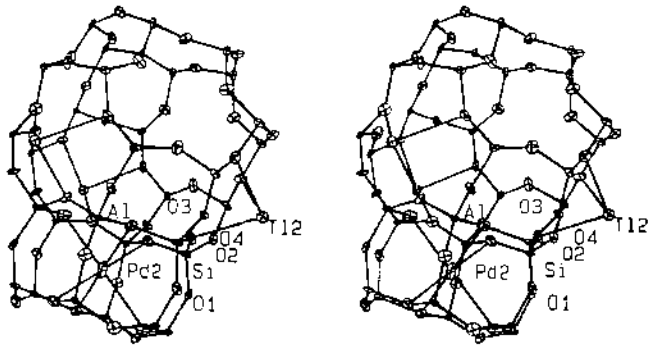

Figure 4. Stereoview of a sodalite cavity with an attached D6R in dehydrated $Pd_{21}Tl_{50}$-X. One Pd^{2+} ion at Pd(2) (site I) and three Tl^- ions at Tl(2) (site II) are shown. About 12.5% of sodalite cavities can have this arrangement. About 50% of sodalite cavities have three Pd^{2-} ions at Pd(1) (site I′), one Tl^+ ion at Tl(1) (site I′), and three Tl^- ions at Tl(2) (site II). Ellipsoids of 20% probability are shown.

plane. The Pd(1)-O(3) bond distance, 2.10(1) Å, is almost the same as the sum of the ionic radii of Pd^{2-} and O^{2-}, 2.18 Å (0.86 + 1.32).[26] The O(3)-Pd(1)-O(3) bond angle of 119.9(6)°, which is almost ideal trigonal planar, indicates that the Pd^{2+} ion fits the six-ring well. The Tl(1)-O(3) bond distance, 2.59(1) Å, is less than the sum of the ionic radii of Tl^- and O^{2-}, 2.79 Å (1.47 + 1.32).[26] Approximately two Tl^+ ions at Tl(1), consistent with the observed occupancy at averaged positions (see Table 1), can lie at two adjacent I′ sites in the same β-cage. The strong electrostatic repulsion between two large and adjacent Tl^- cations at Tl(1) and between Tl(1) and Pd(1) cations can push each other to the charged oxygen planes. The short Tl(1)-O(3) bond distance suggests this phenomenon and a bond with some covalent nature.

About 27 Tl^- ions at Tl(2) occupy the 32-fold site II in a supercage. Each Tl(2) ion coordinates trigonally at 2.82(1) Å to three O(2) framework oxygens and is recessed *ca.* 1.74 Å into the supercage from its O(2) plane (see Figure 3). Tl-O bond distance, 2.82(1) Å, is nearly the same as the sum of the ionic radii of Tl^+ and O^{2-}, 2.79 Å.[26] The fifteen Tl^+ ions at Tl(3) and Tl(4) occupy two different 96-fold site III′ in the supercage, with occupancies of 11 and 4, respectively. The bond distances of Tl-O (Tl(3)-O(4): 2.75(2) and 3.02(2) Å, Tl(4)-O(1): 3.03(4) and 3.07(4) Å) are similar to those found in dehydrated $Cd_{24.5}Tl_{43}$-X[7] and $Sr_{8.5}Tl_{75}$-X.[22] It can be illustrated that the large Tl^+ ions form ionic bonds with framework oxygens when they are in the supercage, whereas they show some covalent character in the sodalite cage.

$Pd_{21}Tl_{50}$-X: In this structure, twenty-one Pd^{2-} ions occupy two different crystallographic sites, and fifty Tl^- ions occupy four different sites. Though the mole ratio of Pd^{2-} to Tl^- was as high as 200 : 1, only about 46% of the total cations were exchanged by Pd^{2-} ions. Twenty Pd^{2-} ions at Pd(1) preferentially occupy site I′, and one Pd^{2+} ion at Pd(2) occupies octahedral site I, at the center of D6R (see Figure 4). The octahedral Pd(2)-O(3) distance, 2.71(2) Å, is much longer than the sum of the ionic radii of Pd^{2+} and O^{2-}, 2.18 Å.[26] Because every site I is surrounded by two I′ sites, the neighboring positions of I and I′ cannot be occupied simultaneously because of the strong electrostatic repulsion between ions. Thus, the site occupation of the linked group I + I′ cannot exceed 32, namely, $n(\mathrm{I}) - n(\mathrm{I}')/2 \leq 16$, where $n(\mathrm{I})$ and $n(\mathrm{I}')$ are the number of cations in each site per unit cell. From this relationship, the observed cation populations of the remaining site I′ are equal to ten. The remaining ten I′ sites are filled by Tl^+ ions at Tl(1). About 62.5% of the sodalite cages can contain one Tl^- ion at Tl(1) and three Pd^{2-} ions at Pd(1). About 25% contains two Tl(1) and two Pd(1)

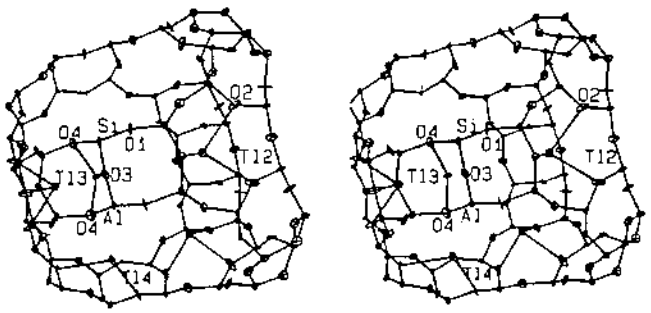

Figure 3. Stereoview of the supercage of dehydrated $Pd_{18}Tl_{56}$-X. Three Tl^+ ions at Tl(2) (site II), one Tl^+ ion at Tl(3) (site III′), and one Tl^+ ion at Tl(4) (site III′) are shown. About 25% of supercages can have this arrangement. Ellipsoids of 20% probability are used.

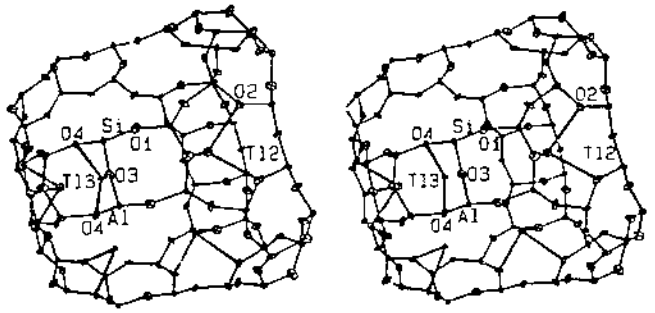

Figure 5. Stereoview of the supercage of dehydrated $Pd_{21}Tl_{50}$-X. Three Tl^- ions at Tl(2) (site II) and two Tl^+ ions at Tl(3) (site III′) are shown. About 50% of supercages can have this arrangement. Ellipsoids of 20% probability are used.

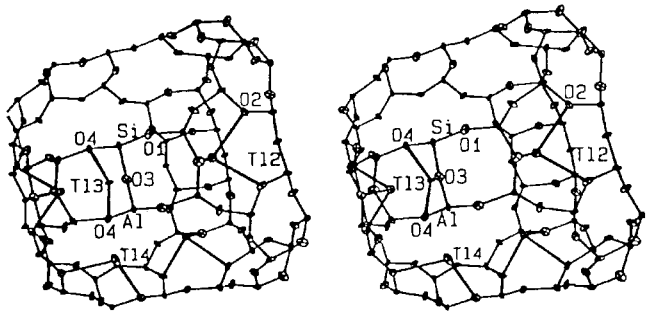

Figure 6. Stereoview of the supercage of dehydrated $Pd_{21}Tl_{50}$-X. Three Tl^+ ions at Tl(2) (site II), one Tl^+ ion at Tl(3) (site III′), and one Tl^+ ion at Tl(4) (site III′) are shown. About 37.5% of supercages can have this arrangement. Ellipsoids of 20% probability are used.

ions. The remaining 12.5% contains one Pd(1), one Pd(2) at site I, and one Tl(1). Each Pd(1) and Tl(1) is recessed *ca.* 0.06(1) Å and 1.52(1) Å, respectively, into the sodalite unit from the three O(3) plane, almost the same as in $Pd_{18}Tl_{56}$-X. Pd^{2-} and Tl^- ions at site I′ coordinates at 2.08(2) and 2.58(2) Å, respectively, to the three O(3) oxygens (see Figure 4). The Pd(1)-O(3) bond distance, 2.08(2) Å, is almost the same as the sum of the ionic radii of Pd^{2-} and O^{2-}, 2.18 Å.[26] The O(3)-Pd(1)-O(3) bond angle of 119.9(7)°, which is almost ideal trigonal planar, indicates that the Pd^{2-} ion fits this six-ring well. The Tl(1)-O(3) bond distance, 2.58(2) Å, is less than the sum of the ionic radii of Tl^- and O^{2-}, 2.79 Å.[26] As in $Pd_{18}Tl_{56}$-X, the strong ionic repulsions between two Tl(1) cations or between Tl(1) and Pd(1) cations at I′ sites may push each other to the charged oxygen planes. The short Tl(1)-O(3) bond distance suggests this phenomenon and some covalent character of the bond.

Table 3. Deviations (Å) of Cations from Six-Ring Planes

	$Pd_{18}Tl_{56}$-X	$Pd_{21}Tl_{50}$-X
At O(3)[a]		
Pd(1)	0.07(1)	0.06(1)
Pd(2)		-1.74(1)
Tl(1)	1.52(1)	1.52(1)
At O(2)[b]		
Tl(2)	1.74(1)	1.77(1)

[a]The negative and positive deviations indicate that the atom lies in D6R and sodalite cavity, respectively. [b]A positive deviation indicates that the atom lies in the supercage.

Table 4. Distribution of Nonframework Atoms over Sites

Sites	Crystals	
	$Pd_{18}Tl_{56}$-X	$Pd_{21}Tl_{50}$-X
I		1Pd(2)
I′	18Pd(1)	20Pd(1)
	14Tl(1)	10Tl(1)
II	27Tl(2)	23Tl(2)
III′	11Tl(3)	13Tl(3)
	4Tl(4)	4Tl(4)

Twenty-three Tl^+ ions at Tl(2) lie at site II. Tl(2) is recessed *ca.* 1.77(1) Å into the supercage from the S6R plane at O(2) (see Figures 5 and 6). Each of these Tl^- ions coordinates to three O(2) oxygens at 2.82(2) Å, nearly equal to the sum of the corresponding ionic radii, 2.79 Å. The angle at Tl(2), O(2)-Tl(2)-O(2), is *ca.* 84.7(6)°, far less than the trigonal planar, indicating again that the Tl^+ ion is too large to fit into the plane of this six-ring. The seventeen Tl^+ ions at Tl(3) and Tl(4) lie in the supercage at two different III′ sites with occupancies of 13 and 4, respectively. The bond distances of Tl-O (Tl(3)-O(4): 2.83(3) and 2.97(3) Å. Tl(4)-O(1): 2.98(7) and 3.15(7) Å) are similar to those found in dehydrated $Pd_{18}Tl_{56}$-X. It shows that the Tl^+ ions at Tl(3) and Tl(4) form loose ionic bonds with framework oxygens of O(1) and O(4).

The present work indicates that all of the Na^- ions in zeolite X can be replaced by Pd^{2-} and Tl^- ions. However, the exchange of Pd^{2-} ions was limited to about 46%. Both in $Pd_{18}Tl_{56}$-X and $Pd_{21}Tl_{50}$-X structures, Pd^{2+} ions prefer to locate at site I′, with occupancies of 18 and 20, respectively. These Pd^{2-} ions at site I′ fit the double six-ring plane well, nearly ideal trigonal planar. In the $Pd_{21}Tl_{50}$-X structure, one Pd^{2+} ion was found at site I. The Tl^+ ions fill the remaining I′ sites and then occupy site II and two different III′ sites. Because the Tl^+ ion is too large to fit into the double or single six-ring planes, it is recessed a long distance into the sodalite cavity or into the supercage. However, the bond distance of Tl-O is somewhat different, depending on whether the Tl^- ion is in the sodalite cavity or in the supercage. Tl^- ions form ionic bonds with adjacent oxygens, but they show some covalent character in Tl-O bonds when they are in the sodalite cavities.

Acknowledgment. This work was supported by the Brain Korea 21 Project, 2000.

Supporting Information Available: Tables of calculated and observed structure factors (8 pages). The supporting materials will be given upon your request to the correspondence author (Fax: +82-51-516-7421; e-mail: ykim@hyowon.pusan.ac.kr).

References

1. Rabo, J. A. *Zeolite Chemistry and Catalysis*, ACS Monograph No. 171; 1976.
2. Breck, D. W. *Zeolite Molecular Sieves*; Wiley Jones: New York, 1974.
3. Lee, H. S.; Cruz, W. V.; Seff, K. *J. Phys. Chem.* **1982**, *86*, 3562.
4. Heo, N. H.; Patlinghug, W. C.; Seff, K. *J. Phys. Chem.* **1986**, *90*, 3931.
5. Patlinghug, W. C.; Seff, K. *J. Phys. Chem.* **1990**, *94*, 7662.
6. Jang, S. B.; Jeong, M. S.; Kim, Y.; Seff, K. *J. Phys. Chem. B* **1997**, *101*, 9041.
7. Kwon, J. H.; Jang, S. B.; Kim, Y. *J. Phys. Chem.* **1996**, *100*, 13720.
8. McCusker, L. B.; Seff, K. *J. Phys. Chem.* **1981**, *85*, 405.
9. Ronay, C.; Seff, K. *Zeolites* **1993**, *13*, 97.
10. Pigras, F.; Gonez, R. *Molecular Sieves*; Am. Chem. Soc.:

Washington, D. C., 1973; p 480.
11. Gallezot, P. *Catal. Rev. Sci. Eng.* **1979**, *201*, 121.
12. Gallezot, P. *Stud. Surface Catal.* **1980**, *5*, 129.
13. Sauvage, A.; Massian, P. *J. Chem. Soc. Faraday Trans.* **1995**, *91*, 3291.
14. Bergeret, G.; Gallezot, P.; Imelik, B. *J. Phys. Chem.* **1981**, *85*, 411.
15. Gallezot, P.; Imelik, B. *Advan. Chem. Ser.* **1973**, *121*, 66.
16. Gallezot, P.; Imelik, B. *Molecular Sieves*; Am. Chem. Soc.: Washington, D.C., 1973; p 66.
17. Homeyer, S. T.; Sachtler, W. M. H. *J. Catal.* **1989**, *117*, 91.
18. Lee, S. H.; Kim, Y.; Seff, K. *J. Phys. Chem. B* **2000**, *104*, 2490.
19. Kim, Y.; Han, Y. W.; Seff, K. *Zeolites* **1997**, *18*, 325.
20. Jang, S. B.; Song, S. H.; Kim, Y. *J. Korean Chem. Soc.* **1995**, *39*, 1.
21. Jang, S. B.; Kim, M. S.; Han,Y. W.; Kim, Y. *Bull. Korean Chem. Soc.* **1996**, *17*, 7.
22. Kim, M. J.; Kim, Y.; Seff, K. *Korean J. Crystallography* **1997**, *8*, 1.
23. Bogomolov, V. N.; Petranovskii, V. P. *Zeolites* **1986**, *6*, 418.
24. *International Tables for X-Ray Crystallography*; Kynoch Press: Birmingham, England, 1974; Vol. II, p 302.
25. Yeom, Y. H.; Kim, Y.; Song, S. H.; Seff, K. *J. Phys. Chem. B* **1997**, *101*, 6914.
26. *Handbook of Chemistry and Physics, 70th ed.*; The Chemical Rubber Co.: Cleveland, Ohio, 1989/1990; p F-187.
27. *MolEN*, a structure determination package supplied by Enraf-Nonius, Netherlands, 1990.
28. *International Tables for X-ray Crystallography*; Kynoch Press: Birmingham, England, 1974; Vol IV, p 73.
29. Cromer, D. T. *Acta Crystallogr.* **1965**, *18*, 17.
30. reference 28, p 149.
31. Sun, T.; Seff, K.; Heo, N. H.; Petranovskii, V. P. *Science* **1993**, *259*, 495.
32. Sun, T.; Seff, K. *Chem. Rev.* **1994**, *94*, 859.